Electronic Supplementary Material (ESI) for Physical Chemistry Chemical Physics.

Supporting Information for:

Shifted Equilibria of Organic Acids and Bases in the Aqueous Surface Region

Josephina Werner,[a,b,*] Ingmar Persson,[b] Olle Björneholm,[a] Delphine Kawecki,[a,†]
Clara-Magdalena Saak,[a] Marie-Madeleine Walz,[a,§] Victor Ekholm,[a] Isaak Unger,[a]
Corina Valtl,[a] Carl Caleman,[a,c] Gunnar Öhrwall[d] and Nønne L. Prisle[e,f]

[a] Department of Physics and Astronomy, Uppsala University, Box 516, SE-751 20 Uppsala, Sweden.

[b] Department of Molecular Sciences, Swedish University of Agricultural Sciences, Box 7015, SE-750 07 Uppsala, Sweden.

[c] Center for Free-Electron Laser Science, Deutsches Elektronen-Synchrotron, Notkestraße 85 DE-22607 Hamburg Germany.

[d] MAX IV Laboratory, Lund University, Box 118, SE-22100 Lund, Sweden.

[e] Faculty of Science, Nano and Molecular Systems Research Unit, Box 3000, FI-90014 University of Oulu, Finland.

[f] Department of Physics, Division of Atmospheric Science, Box 64, FI-00014 University of Helsinki, Finland

[†] Present address: Technology and Society Laboratory, Empa - Swiss Federal Laboratories for Materials Science and Technology, St. Gallen, Switzerland

[§] Present address: Department of Cell and Molecular Biology, Uppsala University, Box 596, SE-75124 Uppsala, Sweden.

[*] Corresponding author

1. MD simulations: computational details and results

Molecular dynamics simulations of the four organic molecules on the vacuum-water interphase were performed using the GROMACS simulation suite,[1] and the generalized amber force field (GAFF)[2] parameters for the molecules in combination with the TIP3P water model. The choice of force field is based on earlier experience which indicate that the combination of GAFF with TIP3P is suited for simulations of organic molecules on water surfaces[3]. In earlier studies[4] we have compared simulations done with the GAFF/TIP3P combination to simulations done using the OPLS/AA force field[2,5,6] together with the SPC water model.[7] These comparisons showed that the dynamics of the organic molecules on water surfaces were described similarly independent of choice of force field parameters.

Force field parameters for the four organic molecules were constructed according to the scheme described in earlier publications.[8,9] To generate the simulation box, one organic molecule was solvated in a 3x3x3 nm^3 box of water. Vacuum-water interphases were introduced by extending one of the axis on both sides of the simulation box to a total length of 9 nm. The final simulation box contained one organic molecule and around 900 water molecules. First a 2 ns equilibration simulation was performed, where the total energy of the system was monitored. The following production run, from where the analysis was done, was 4 ns long.

As in earlier studies[4] a 1.1 nm cutoff was used for both the Lennard-Jones interactions and the switching distance for the particle mesh Ewald (PME) algorithm for the Coulomb interactions.[10,11] The temperature was set to 283 K, and was kept using the Berendsen temperature coupling algorithm, and a coupling constant of 0.1 ps.[12] The LINCS algorithm was used to constrain the bonds[13,14] and periodic boundary conditions were applied.

Resulting density profiles are shown in Figure S1. Snapshots of MD simulations of the studied compounds are shown in Figure S2. The average number of hydrogen bonds that the functional group of each species has with the solvating water molecules was extracted. It was found that the carboxylic acid group of butyric acid forms on average 3.1±0.9 hydrogen bonds. Its charged conjugate forms on average 6.7±0.9. The amine group of *n*-hexyl amine forms on average 2.4±0.9 hydrogen bonds, while the ammonium group forms 2.8±0.5. Furthermore, the density peak close to the aqueous interface was used to estimate the thickness of the surface region in the same way as it was suggested in Ref.[15], i.e. by determining its full-width-at-half-maximum (FWHM). The results are listed in Table S1.

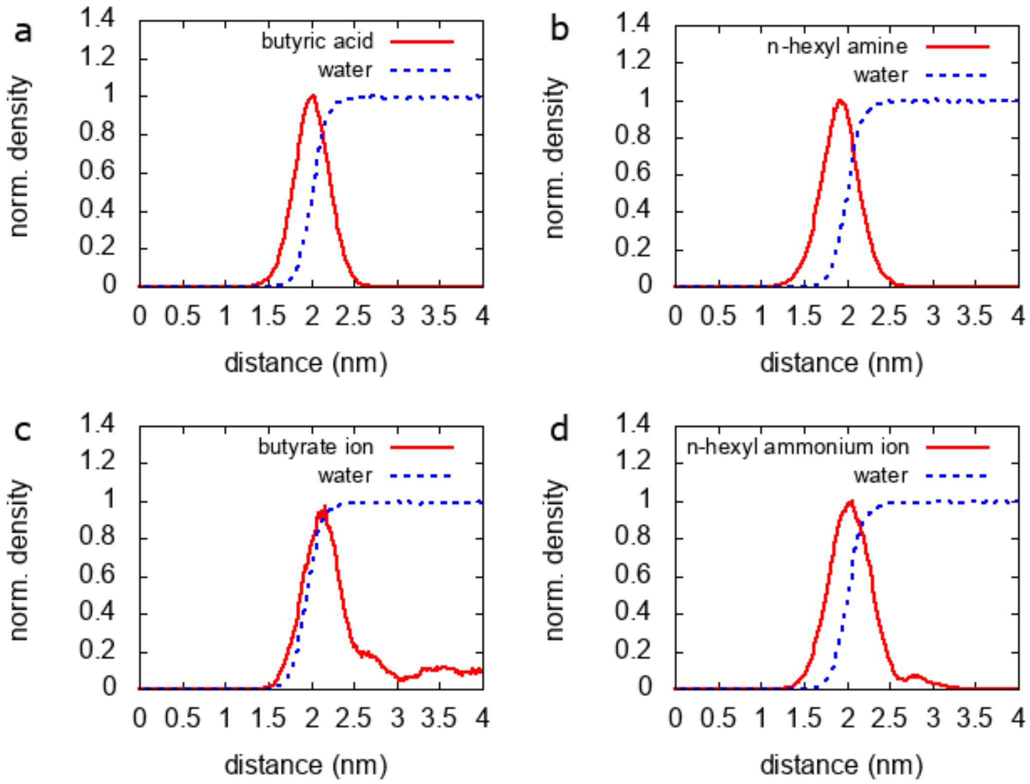

Figure S1 Density profiles as a function of distance from the slab-center. a/ Butyric acid in water; b/ *n*-hexyl amine; c/ butyrate ion; d/ n-hexyl ammonium ion.

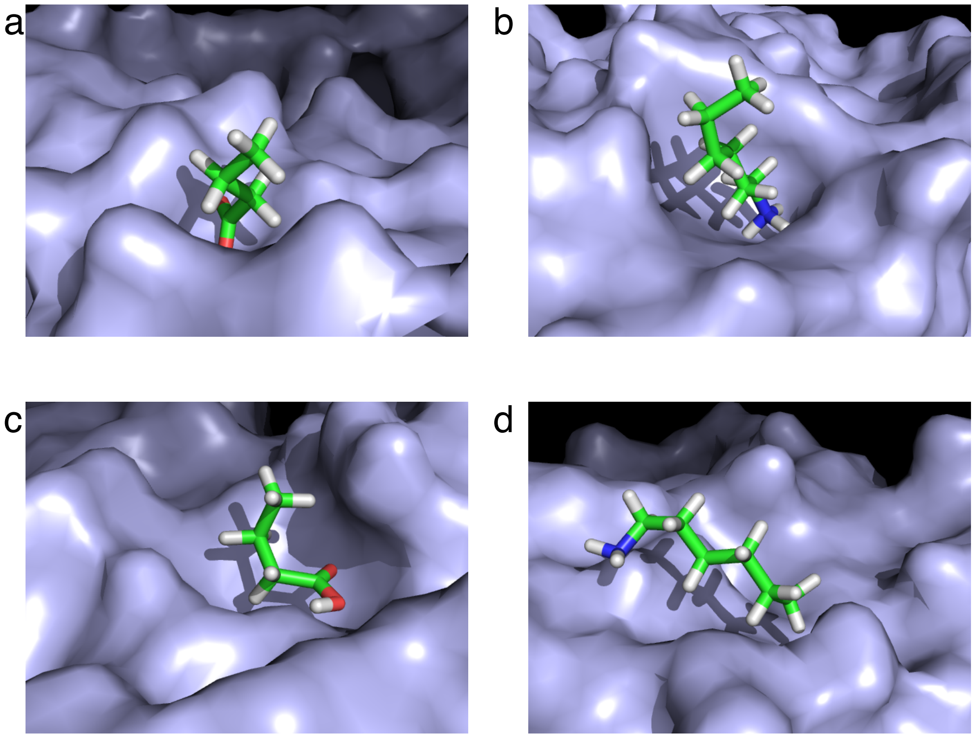

Figure S2 Snapshots of MD simulations of a/ a butyrate ion; b/ a n-hexyl ammonium ion; c/ a butyric acid; d/ a *n*-hexyl amine.

2. Analysis of XPS results

All core-level spectra of aqueous solutions were energy calibrated to the liquid water $1b_1$ binding energy level at 11.16 eV.[16] The core-level spectra were fitted using a minimum number of Voigt profiles, where fit parameters, such as peak areas and binding energies, were extracted for further analysis. During the fitting procedures, the energy positions of the functional groups were linked for each compound and concentration. The Lorentzian full-width-at-half-maximum (FWHM) of C 1s PE lines was set to 0.10 eV, of N 1s PE lines to 0.13 eV[17] and Gaussian FWHM's were linked within each measurement series. Gas phase spectra were also acquired for compounds with considerable volatility (C4H, A4 and A6) by lowering the liquid jet out of the photon beam. These spectra were used to constrain the binding energy splitting and intensity ratios of gas phase contributions to spectra of aqueous solutions during the fitting procedure. An example spectrum showing all fit contributions is shown in Figure S3.

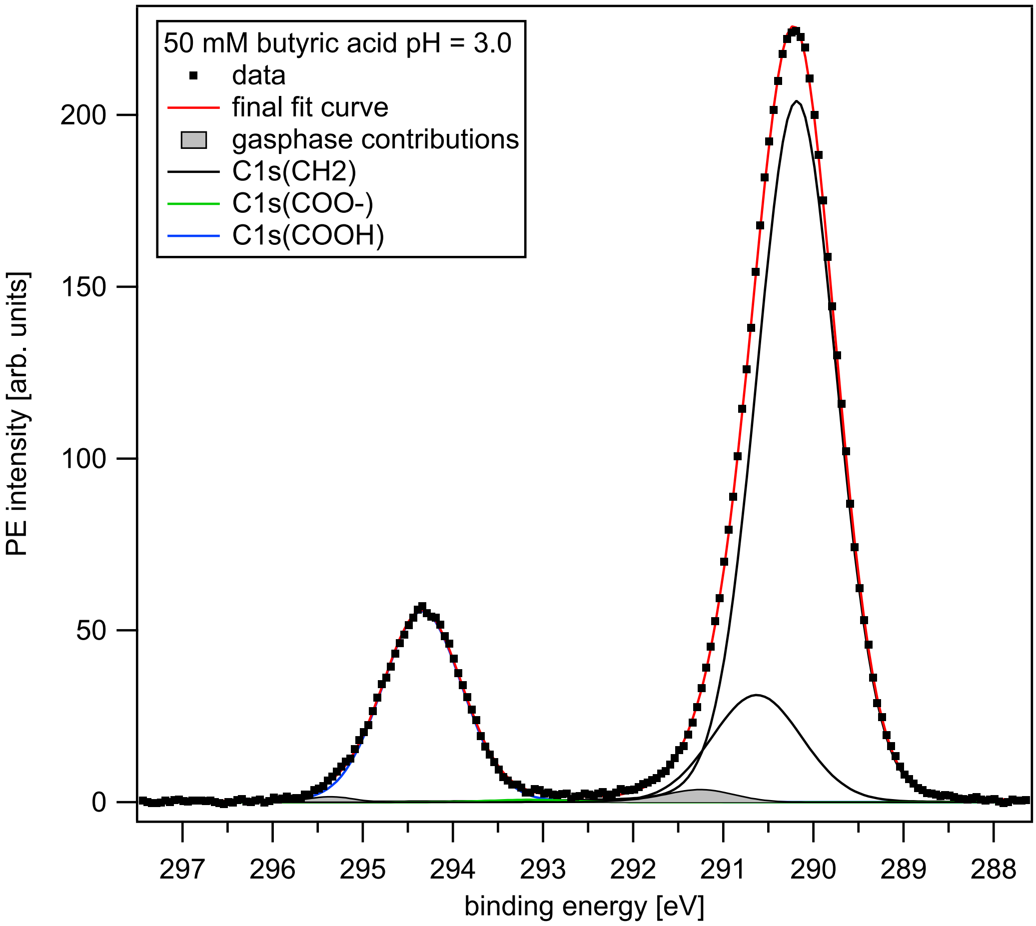

Figure S3 Example spectra of butyric acid at pH = 3.0 showing all fit contributions.

3. Simple two-layer model to quantify surface concentrations from XPS results and MD simulations

Photoemission (PE) intensities of photoelectrons with a given kinetic energy are directly proportional to the concentration of the studied species in the probed volume and its photoionization cross-section, but exponentially attenuated along its path. When similar species are studied at the same experimental conditions (kinetic energy, line up of the spectrometer and the light source etc.), the ratios of PE intensities yield information on the respective spatial distance of the different species from the air-water interface, which is usually referred to as a compound's surface propensity. Surface-active compounds tend to accumulate in the surface region. Hence, the compound's surface concentration (c_s) is higher than the one in the bulk solution (c_b). As the surface sensitivity of XPS is not known exactly, mostly due to uncertainties in the photoelectron's effective attenuation length (EAL) in aqueous solutions and the dimensions of the surface region, surface concentrations of a species in aqueous solution can only be roughly estimated. To do so, a simple two-layer model is introduced, which describes an aqueous solution as being divided into a surface and a bulk region.[15,18] Surface enrichment factors c_s/c_b can be estimated from ratios of a PE signal recorded from a surface-active compound (I_{tot}) and a compound that strictly avoids the surface region (I_b).

$$\frac{c_s}{c_b} = \frac{n_b}{n_s} \cdot \left(\frac{I_{tot}}{I_b} - 1\right) \qquad (1)$$

n_b/n_s is the so-called sensitivity factor, that describes the surface sensitivity of XPS experiments. It can be approximated in different ways.

i) A conservative estimate for the sensitivity assumes that the surface region contributes with 50 ± 25 % to the total recorded signal. This yields surface sensitivity factors of $0.333 < n_b/n_s < 3$.[15,18,19]

ii) In an earlier work[15] a more refined approach was suggested, where results from MD simulations are used to estimate the thickness of the surface region. Assuming the surface region expands between $0 \leq z \leq D$, while the bulk of the solution stretches from $D < z \leq \infty$, the surface sensitivity of XPS can be expressed as follows, see supporting information (SI) of Ref. 15 for details.

$$\frac{n_b}{n_s} = \frac{EAL \cdot e^{-\frac{D}{EAL}}}{EAL \cdot (1 - e^{-\frac{D}{EAL}})} \,. \qquad (2)$$

iii) In this earlier work[15] it was also shown that $n_b/n_s \approx 1.27$ (44% surface contribution) gives best overlap between modeled surface tension using XPS results and experimentally determined surface tension values for the case of succinic acid measured with a kinetic energy of roughly 70 eV. The same value has been reported by Olivieri et al.,[20] using a completely different approach.

For this work, we estimated the surface thickness from results of MD simulations and by assuming the surface region to be equally thick as the length of studied compound in all-trans configuration.[21] The assumed thicknesses, the resulting sensitivity factors and portion of the PE signal originating from the surface region are listed in Table S1. Here we assumed that the EAL is 10 Å.[22]

Table S1 Estimated surface thicknesses for the studied compounds from MD simulations and resulting sensitivity factors.

compound	**surface thickness (from MD)**	n_b/n_s	***portion of the PE signal from the surface***
butyric acid	4.0 Å	2.03	33%
butyrate ions	4.7 Å	1.67	38%
hexylamine	4.3 Å	1.86	35%
hexylammonium ions	4.9 Å	1.58	39%

compound	***length of molecule in all-trans configuration***	n_b/n_s	***portion of the PE signal from the surface***
butyric acid	4.5 Å	1.78	36%
butyrate ions	4.4 Å	1.81	36%
hexylamine	6.7 Å	1.05	49%
hexylammonium ions	6.8 Å	1.03	49%

Using the different approaches, the portion of the PE signal from the surface yields values between 33 and 49%. The larger the surface contribution, the lower the sensitivity factor, resulting in overall smaller surface concentration values. We decided to use a sensitivity factor of 1, i.e. 50% surface contribution, for all surface concentration estimations. Hence, the estimated surface concentrations can be regarded as on the lower limit.

3. Langmuir adsorption model applied to results of XPS experiments

A Langmuir adsorption based model has been previously applied to results of XPS experiments.[21,23,24] It enables the estimation of surface coverage, surface concentrations as well as the free energy of adsorption ΔG_{ads}, which is a measure of the net energy gain for a solution with a single solute partially accumulated at the interface. A form of the Langmuir adsorption isotherm is used to fit results of XPS experiments, which describes the surface component I_s of the total recorded PE signal I_{tot} as a function of the bulk mole fraction x_{bulk} of a compound in aqueous solution.

$$I_s = \frac{I_{s,max} x_{bulk}}{x_{bulk} + (1 - x_{bulk}) exp\left(\frac{\Delta G_{ads}}{RT}\right)} \qquad (3)$$

While I_s scales with the surface concentration of the dissolved compound c_s, $I_{s,max}$ is directly proportional to the maximum surface concentration $c_{s,max}$. The ratio of I_s and $I_{s,max}$ gives the surface coverage p.

$$p = I_s / I_{s,max} = c_s / c_{\mathrm{s,max}} \qquad (4)$$

R is the universal gas constant and T the absolute temperature, which was set to 283.15 K corresponding to the temperature of the XPS experiments. The surface component of the total recorded signal I_s is calculated by dividing the total recorded signal $\mathrm{I_{tot}}$ by the number of carbon atoms in the corresponding molecule and a bulk reference signal (approximated by means of a reference spectrum of sodium formate for C 1s PE intensities) is subtracted. For further analysis in this study, the maximum surface concentration $c_{s,max}$ is set to be the pure compounds concentration. Hence, by knowing the surface coverage p and the pure compounds concentration, the surface concentration c_s can be estimated for any bulk concentration.

References

1 B. Hess, C. Kutzner, D. van der Spoel and E. Lindahl, *J. Chem. Theory Comput.*, 2008, **4**, 435–447.

2 W. L. Jorgensen, J. Chandrasekhar, J. D. Madura, R. W. Impey and M. L. Klein, *J. Chem. Phys.*, 1983, **79**, 926.

3 J. S. Hub, C. Caleman and D. van der Spoel, *Phys. Chem. Chem. Phys.*, 2012, **14**, 9537–9545.

4 M.-M. Walz, C. Caleman, J. Werner, V. Ekholm, D. Lundberg, N. L. Prisle, G. Öhrwall and O. Björneholm, *Phys. Chem. Chem. Phys.*, 2015, **17**, 14036–14044.

5 W. L. Jorgensen and J. Tirado-Rives, *Proc. Natl. Acad. Sci. U. S. A.*, 2005, **102**, 6665–6670.

6 H. J. C. Berendsen, J. R. Grigera and T. P. Straatsma, *J. Phys. Chem.*, 1987, **91**, 6269–6271.

7 H. J. C. Berendsen, J. P. M. Postma, W. F. van Gunsteren and J. Hermans, Springer Netherlands, 1981, pp. 331–342.

8 D. van der Spoel, P. J. van Maaren and C. Caleman, *Bioinformatics*, 2012, **28**, 752–753.

9 C. Caleman, P. J. van Maaren, M. Hong, J. S. Hub, L. T. Costa and D. van der Spoel, *J. Chem. Theory Comput.*, 2012, **8**, 61–74.

10 T. Darden, D. York and L. Pedersen, *J. Chem. Phys.*, 1993, **98**, 10089.

11 U. Essmann, L. Perera, M. L. Berkowitz, T. Darden, H. Lee and L. G. Pedersen, *J. Chem. Phys.*, 1995, **103**, 8577.

12 H. J. C. Berendsen, J. P. M. Postma, W. F. van Gunsteren, A. DiNola and J. R. Haak, *J. Chem. Phys.*, 1984, **81**, 3684.

13 B. Hess, *J. Chem. Theory Comput.*, 2007, **4**, 116–122.

14 W. F. Van Gunsteren and H. J. C. Berendsen, *Mol. Simul.*, 1988, **1**, 173–185.

15 J. Werner, J. Julin, M. Dalirian, N. L. Prisle, G. Ohrwall, I. Persson, O. Björneholm, I. Riipinen, G. Öhrwall, I. Persson, O. Björneholm and I. Riipinen, *Phys. Chem. Chem. Phys.*, 2014, **16**, 21486–21495.

16 B. Winter, R. Weber, W. Widdra, M. Dittmar, M. Faubel and I. V Hertel, *J. Phys. Chem. A*, 2004, **108**, 2625–2632.

17 J. L. Campbell and T. Papp, *At. Data Nucl. Data Tables*, 2001, **77**, 1–56.

18 N. L. Prisle, N. Ottosson, G. Öhrwall, J. Söderström, M. Dal Maso and O. Björneholm, *Atmos. Chem. Phys.*, 2012, **12**, 12227–12242.

19 C. J. Powell and A. Jablonski, *Nucl. Instruments Methods Phys. Res. A*, 2009, **601**, 54–65.

20 G. Olivieri, K. M. Parry, C. J. Powell, D. J. Tobias and M. A. Brown, *J. Chem. Phys.*, 2016, **144**, 154704.

21 M.-M. M.-M. Walz, J. Werner, V. Ekholm, N. L. Prisle, G. Öhrwall and O. Björneholm, *Phys. Chem. Chem. Phys.*, 2016, **18**, 6648–6656.

22 H. Nikjoo, S. Uehara, D. Emfietzoglou and A. Brahme, *New J. Phys.*, 2008, **10**, 1–28.

23 K. A. Perrine, M. H. C. Van Spyk, A. M. Margarella, B. Winter, M. Faubel, H. Bluhm and J. C. Hemminger, *J. Phys. Chem. C*, 2014, **118**, 29378–29388.

24 J. Werner, M. Dalirian, M.-M. Walz, V. Ekholm, U. Wideqvist, S. J. Lowe, G. Öhrwall, I. Persson, I. Riipinen and O. Björneholm, 2016, **50**, 7434–7442.